Optimization of Energy Dissipation Rate in Structures

Vernon H. Neubert
Professor of Engineering Science and Mechanics
133 Hammond Building
The Pennsylvania State University
University Park, PA, 16802

ABSTRACT

The present paper deals with the control of free vibrations in structures by maximizing the energy dissipation rate, or minimizing the settling time of transient free vibrations. The energy dissipation rate is a generalization of the Rayleigh dissipation function for viscous damping. Both proportional and nonproportional damping are included and the eigenvalues and eigenvectors are complex in general. The dissipation rate D is a real, positive number and the integral of 2D with respect to time represents the total dissipated energy for the specified time interval, which is of primary interest in designing damping treatments.

It is shown that, for free vibrations, the value of D at time t=0 is sufficient information to optimize the dissipation rate, so that integration over a time period is not necessary. The dissipation rate for each mode, or a set of appropriately weighted modes, becomes the objective function. The optimum location for a limited amount of damping is determined.

Particular examples of the optimization of damping are given for a truss having ten bars. It is assumed that viscous damping is to be added to only the truss members where it will be most useful and an appropriate constraint equation is written. To carry out the optimization, the sensitivities may be determined for the eigenvalues and the eigenvectors by taking their derivatives with respect to the dashpot constants in the matrix $\mathbb{C}$. The sensitivity of D may be determined by finite differences or more precisely using the eigenvalue and eigenvector derivatives. Optimization of the dissipation rate D is compared with optimization of the modal damping ratios. Results are related to settling time. Thus the problem is formulated so it can be solved by an optimization procedure, such as the Method of Feasible Directions.

A phenomenon of particular interest is demonstrated: namely, that as the damping is increased in certain areas of a structure, the modal damping of an individual mode may decrease dramatically while it increases in other modes. There is an associated change in mode shape, which would not be predicted if proportional damping had been assumed.

Background and Related Literature

Optimal control of vibrations in structures by active or passive means is an important practical problem, as evidenced by titles of conferences[1-4] and published books[5-8]. Passive damping may be developed by the use of dashpots, piezoelectric elements, electromagnetic devices, or viscoelastic layers, to only a few methods. The present paper deals with the optimum choice of size and location of velocity- or rate-dependent linear elements. The analysis has a wide range of applications and applies to viscoelastic damping and to active control where the rate-dependent gains are constant.

Much information is available on the behavior of viscoelastic materials as a function of temperature and frequency[9], but the representation of this behavior in dynamic analyses of structures is a challenging problem because of the variation of the dynamic properties with frequency and temperature. Bagley and Torvik[10] developed a fractional calculus approach to the representation of viscoelastic damping and have adapted it to finite element techniques. A meth-requiring calculation of complex stiffness matrix at each resonant frequency was outlined by Segalman[11] in terms of measurable viscoelastic properties. The use of fictitious, over-damped, mini-oscillators to represent frequency variation of the complex modulus is a part of the method outlined by McTavish and Hughes[12]. Closed-loop, constant gain, rate-dependent active control makes use of dashpots with negative parameters.

To optimize parameters, one needs the derivatives or sensitivities of the response variables in terms of the design parameters. Venkayya[13] presented a unified approach to optimization suitable for application to problems in many disciplines. In addition, computer programs are available, such as CONMIN, by Vanderplaats[14], which will determine optimum values of design parameters using sensitivity and response variable values provided by the program user. Determination of derivatives of eigenvalues and eigenvectors is the subject of papers by Rogers[15], Nelson[16], and others[17-20]. With the assumption of proportional damping, Gibson and Johnson[21] optimize the size and location of viscoelastic damping on plates by optimizing modal loss factor, taken to be the ratio of the modal strain energy in the viscoelastic layer to the total modal strain energy.

ANALYTICAL BASIS

The problem is formulated in the state vector form:

$$\begin{bmatrix} M & 0 \\ 0 & -K \end{bmatrix} \begin{Bmatrix} \ddot{\underline{z}} \\ \dot{\underline{z}} \end{Bmatrix} + \begin{bmatrix} C & K \\ K & 0 \end{bmatrix} \begin{Bmatrix} \dot{\underline{z}} \\ \underline{z} \end{Bmatrix} = \begin{Bmatrix} \underline{p}(t) \\ \underline{0} \end{Bmatrix}$$

or

$$M^* \dot{\underline{\eta}} + K^* \underline{\eta} = \underline{P}(t) \tag{2}$$

The resulting eigenvalue problem is

$$[-\lambda I + A] \underline{x} = 0 \tag{3}$$

where

$$A = -[M^*]^{-1} K^*. \tag{4}$$

The matrices M, K and C are assumed to be symmetric.

The following modal notation is used.

φ_{ji} = the modal displacement vector, Nx1

$\underline{\Psi}_{ji} = \begin{Bmatrix} \lambda_i \varphi_{ji} \\ \varphi_{ji} \end{Bmatrix}$ = state space modal vector, 2Nx1

$\underline{x}$ = displacement vector, nx1

$T = \frac{1}{2} \dot{\underline{x}}^T M \dot{\underline{x}}$ = kinetic energy

$U = \frac{1}{2} \underline{x}^T K \underline{x}$ = potential energy

$D = \frac{1}{2} \dot{\underline{x}}^T C \dot{\underline{x}}$ = half the rate of energy dissipation

$H = T + U$ = the Hamiltonian

Now the energies may be related to the differential equations of motion for free vibrations,

$$M \ddot{\underline{x}} + C \dot{\underline{x}} + K \underline{x} = \underline{F}. \tag{5}$$

Pre-multiplying by $\dot{\underline{x}}^T$, the energies may be identified.

$$\dot{\underline{x}}^T M \ddot{\underline{x}} + \dot{\underline{x}}^T C \dot{\underline{x}} + \dot{\underline{x}}^T K \underline{x} - \dot{\underline{x}}^T \underline{F} = 0 \tag{6}$$

$$\frac{d}{dt}\left[\frac{1}{2} \dot{\underline{x}}^T M \dot{\underline{x}} + \frac{1}{2} \underline{x}^T K \underline{x}\right] + \dot{\underline{x}}^T C \dot{\underline{x}} - \dot{\underline{x}}^T \underline{F} = 0 \tag{7}$$

Thus the rate of change of the Hamiltonian is equal to the rate at which external work is done on the system minus the rate of energy dissipation, or

$$\dot{T} + \dot{U} = \dot{\underline{x}}^T \underline{F} - 2D \tag{8}$$

For conservative systems, the rate of change of the Hamiltonian is zero. If Eq. (8) is integrated with respect to time, energies at time t are related

by

$$H(t) - H(0) = \int_0^t (\dot{\underline{x}}^T \underline{F} - 2D)\, dt \tag{9}$$

Modal Energy, General Viscous Damping

Now for general viscous damping, where Ψ is 2Nx2N and q is 2Nx1, the state vector may be expanded in terms of the modal eigenvectors as

$$\begin{Bmatrix} \dot{x} \\ x \end{Bmatrix} = \Psi \; q \tag{10}$$

$$= \begin{bmatrix} \lambda_1\varphi_1 & \bar{\lambda}_1\bar{\varphi}_1 & \lambda_2\varphi_2 & \lambda_2\bar{\varphi}_2 & \cdot & \cdot & \lambda_n\bar{\varphi}_n \\ \varphi_1 & \bar{\varphi}_1 & \varphi_2 & \bar{\varphi}_2 & & & \varphi_n \end{bmatrix} \begin{Bmatrix} q_1 \\ \bar{q}_1 \\ q_2 \\ \bar{q}_2 \\ \cdot \\ \cdot \\ \bar{q}_n \end{Bmatrix} \tag{11}$$

The free vibration modal amplitudes $q_i(t)$ are, as a function of time t,

$$q_i(t) = A_i \; e^{-\lambda_i t} \tag{12}$$

If the mode is underdamped, then the eigenvalues λ_i are of the form

$$\lambda_i = -\zeta_i\omega_i + j\;\omega_i(1-\zeta_i^2)^{0.5} = -\zeta_i\omega_i + j\omega_{Di} \tag{13}$$

and

$$\lambda_{i+1} = \bar{\lambda}_i = -\zeta_i\omega_i - j\;\omega_i(1-\zeta_i^2)^{0.5} = -\zeta_i\omega_i - j\omega_{Di} \tag{14}$$

For real initial values, the response will be real, the $q_i(t)$ occur in complex conjugate pairs, and $q_{i+1}(t)$ will be

$$q_{i+1}(t) = \bar{q}_i(t) = \bar{A}_i \; e^{-\bar{\lambda}_i t}. \tag{15}$$

The kinetic energy is

$$T = \frac{1}{2}\,\dot{x}^T M \,\dot{x} = \frac{1}{2}\,\dot{q}^T \Phi^T M \,\Phi\, \dot{q} \tag{16}$$

and the derivative of T with respect to time is

or $$\dot{T} = \ddot{q}^T \Phi^T M \,\Phi\, \dot{q}\,. \tag{17}$$

The derivative of the potential energy with respect to time is

$$\dot{U} = \dot{q}^T \Phi^T K \,\Phi\, q \tag{18}$$

and the dissipation function D is

$$2D = \dot{q}^T \Phi \; C \;\Phi\; \dot{q} \tag{19}$$

It is helpful to see the details for a two-degree-of-freedom system.

$$2D = \begin{Bmatrix} \dot{q}_1 \dot{\bar{q}}_1 \dot{q}_2 \dot{\bar{q}}_2 \end{Bmatrix} \begin{bmatrix} \varphi_1^T C\varphi_1 & \varphi_1^T C\bar{\varphi}_1 & \varphi_1^T C\varphi_2 & \varphi_1^T C\bar{\varphi}_2 \\ \bar{\varphi}_1^T C\varphi_1 & \bar{\varphi}_1^T C\bar{\varphi}_1 & \bar{\varphi}_1^T C\varphi_2 & \bar{\varphi}_1^T C\bar{\varphi}_2 \\ \varphi_2^T C\varphi_1 & \varphi_2^T C\bar{\varphi}_1 & \varphi_2^T C\varphi_2 & \varphi_2^T C\bar{\varphi}_2 \\ \bar{\varphi}_2^T C\varphi_1 & \bar{\varphi}_2^T C\bar{\varphi}_1 & \bar{\varphi}_2^T C\varphi_2 & \bar{\varphi}_2^T C\bar{\varphi}_2 \end{bmatrix} \begin{Bmatrix} \dot{q}_1 \\ \dot{\bar{q}}_1 \\ \dot{q}_2 \\ \dot{\bar{q}}_2 \end{Bmatrix} \tag{20}$$

It can be seen that the complex numbers in the core matrix $\Phi^T C \Phi$ matrix occur in complex conjugate pairs, since the numbers in C are real.

The orthogonality relationships are, in terms of the 2Nx1 ψ vectors

$$\psi_s^T M^* \psi_r = 0 \qquad r \neq s$$

$$\text{and} \quad \psi_r M^* \psi_r = b_r \qquad r = s \tag{21}$$

$$\psi_s K^* \psi_r = 0 \qquad r \neq s$$

$$\text{and} \quad \psi_r K^* \psi_r = -\lambda_r b_r \qquad r = s \tag{22}$$

In terms of the Nx1 φ vectors, the orthogonality relationships are

$$\lambda_r \lambda_s \varphi_s^T M \varphi_r - \varphi_s^T K \varphi_r = 0 \qquad r \neq s \tag{23}$$

$$\text{and} \quad \lambda_r^2 \varphi_r M \varphi_r - \varphi_r K \varphi_r = b_r \qquad r = s \tag{24}$$

$$\lambda_r \lambda_s \varphi_s^T C \varphi_r + (\lambda_r + \lambda_s) \varphi_s^T K \varphi_r = 0 \qquad r \neq s \tag{25}$$

$$\text{and} \quad \lambda_r^2 \varphi_r C \varphi_r + 2\lambda_r \varphi_r^T K \varphi_r = -\lambda_r b_r \qquad r = s \tag{26}$$

The Eqs. (23)-(26) may be combined to form alternate, but not independent, orthogonality relationships as

$$\varphi_s^T C \varphi_r + (\lambda_r + \lambda_s) \varphi_s^T M \varphi_r = 0 \qquad r \neq s \tag{27}$$

$$\text{and} \quad \varphi_r^T C \varphi_r + 2\lambda_r \varphi_r^T M \varphi_r = \lambda_r b_r \qquad r = s \tag{28}$$

From Eqs. (25) and (27) a special relationship[22] follows between the rth mode and its complex conjugate, due to the fact that $\lambda_r \bar{\lambda}_r = \omega_r^2$ and $\lambda_r + \bar{\lambda}_r = -2\zeta_r \omega_r$,

$$\text{namely,} \quad \frac{\varphi_r^T C \bar{\varphi}_r}{\varphi_r^T K \varphi_r} = -\frac{2\zeta_r}{\omega_r} \quad \text{and} \quad \frac{\varphi_r^T C \bar{\varphi}_r}{\varphi_r^T M \varphi_r} = -2\zeta_r \omega_r . \tag{29}$$

Choice of Objective Function for Damping Optimization

If we wish to find the optimum damping by an optimization process, it is common to specify an objective function. In modern control theory the perfor-performance index may be of the form, given for example in reference 4.

$$PI = \int_0^t (\{\psi\}^T [Q] \{\psi\} + \{f\}^T [R] \{f\}) dt \tag{30}$$

where
- $\{\psi\}$ = modal vector, 2Nx1
- $\{f\}$ = active control vector, Px1
- $[Q]$ = state weighting matrix, positive semidefinite
- $[R]$ = control weighting matrix, positive definite

If emphasis is to be placed on particular response or control points, the weighting matrices [Q] and [R] may be so adjusted. In the absence of that type of goal, then [Q] and [R] may be chosen as the unit or identity matrix. In choosing [Q] we might also consider the matrices

$$K^* = \begin{bmatrix} C & K \\ K & 0 \end{bmatrix} \quad CK^* = \begin{bmatrix} C & 0 \\ 0 & 0 \end{bmatrix} \quad KK^* = \begin{bmatrix} 0 & K \\ K & 0 \end{bmatrix} \quad M^* = \begin{bmatrix} M & 0 \\ 0 & -K \end{bmatrix} \tag{31}$$

$$\text{where } K^* = CK^* + KK^*$$

$$\text{Then } \Psi^T K^* \Psi = \Psi^T CK^* \Psi + \Psi^T KK^* \Psi \tag{32}$$

$$= \Lambda^T \Phi^T C \Phi \Lambda + \Psi^T KK^* \Psi \tag{33}$$

and $\Phi^T C \Phi$ and $\Phi^T KK^* \Phi$ are not diagonal, even though $\Phi^T K^* \Phi$ is diagonal. Products $\varphi_i^T C \varphi_i$ appear on the diagonal of $\Phi^T C \Phi$, but off the diagonal terms like $\varphi_j^T C \varphi_i$ occur which are not zero, and in fact may be of the same magnitude as the diagonal terms.

The product $\Psi^T CK^* \Psi$ is important, because it is the kernel of the Rayleigh dissipation function D, as seen in Eq. (34). Note that Φ is Nx2N and C is NxN.

$$2D = \dot{q}^T \Phi^T C \Phi \, \dot{q} = q^T \Lambda \, \Phi^T C \Phi \, \Lambda q \tag{34}$$

The Rayleigh Dissipation Rate as an Objective Function

The Rayleigh Dissipation Function D is given by

$$2D = \dot{x}^T \, C \, \dot{x} \tag{35}$$

In state vector form, the velocity and displacement are expressed in terms of modal coordinates by

$$\underset{2N\times1}{\begin{Bmatrix} \dot{x} \\ x \end{Bmatrix}} = \underset{2N\times2N}{\Psi} \underset{2N\times1}{\begin{Bmatrix} q \end{Bmatrix}} = \begin{bmatrix} \Phi\Lambda \\ \Phi \end{bmatrix} \begin{Bmatrix} q \end{Bmatrix} \tag{36}$$

Hence the dissipation function may be gotten from the product

$$2D = \begin{Bmatrix} \dot{x} \\ x \end{Bmatrix}^T \begin{bmatrix} C & 0 \\ 0 & 0 \end{bmatrix} \begin{Bmatrix} \dot{x} \\ x \end{Bmatrix} = q^T \Psi^T CK^* \Psi q \tag{37}$$

The dissipation function D is a real, positive number. There are 2N modal coordinates, $q_i(t)$, in the form of N complex conjugate pairs. The initial values $q_i(0)$ are gotten from the initial value vectors $\dot{x}(0)$ and $x(0)$. An efficient approach is to use the orthogonality relationship Eq. (21) so that

$$\Psi^T M^* \begin{Bmatrix} \dot{x}(0) \\ x(0) \end{Bmatrix} = B^D q(0). \tag{38}$$

Here B^D is a diagonal matrix of b_r's and the eigenvectors have been normalized so that each B^D=I, the identity matrix. From Eq. (36) we see that if $\underline{q}(0)$ is real, then $\underline{x}(0)$ is real. If we wanted to excite a pure second mode, for example, the following relationships would exist from Eq. (38)

$$\left\{\Psi_1^T\ \bar{\Psi}_1^T\ \Psi_2^T\ \bar{\Psi}_2^T\ \cdots\right\}\left[\ M^*\ \right]\left\{\Psi_2+\bar{\Psi}_2\right\} = \left\{\begin{matrix} q_1(0)\\ \bar{q}_1(0)\\ q_2(0)\\ \bar{q}_2(0)\end{matrix}\right\} = \left\{\begin{matrix}0\\0\\1\\1\\ \vdots\end{matrix}\right\} \tag{39}$$

The vector $\Psi_2+\bar{\Psi}_2$ is real, and Eq. (39) shows that the initial value vector is a pure 2*nd* modal vector when $q_2(0)=\bar{q}_2(0)=1$. This idea will be used next in finding the dissipation function D when we wish to excite a pure mode or group of modes.

It may be observed that an upper bound on the dissipation rate at t=0 can be determined by taking the sum of the absolute values of the real parts of the numbers in the complex matrix $\Psi^T CK^*\Psi$. The sum is then a candidate for an an objective function, to be maximized, in a free vibration problem. It may appear that the magnitude of the dissipation rate is somewhat arbitrary, but it should be noted that because of the normalization of the eigenvectors by $\Psi^T M^*\Psi = B^D = I$, then the initial value of the energy $T(0)-U(0) = 2n$, where n is the number of modes excited. In the examples given below, the initial potential energy U(0) is very small, so the settling time depends on the time it takes the energy level given in Eq. (40) to reach zero. This equation also

$$T(0)+U(0)-\int_0^t 2D\ dt \cong 2n - \int_0^t 2D\ dt \tag{40}$$

shows that the settling time depends simply on the time for 2D to reach zero.

Sensitivity of the Rayleigh Dissipation Function

The sensitivity of the dissipation rate D is gotten by taking the partial derivative $\partial D/\partial C_m$, where C_m is the value of the mth dashpot parameter, and D may be taken in the following form,

$$2D = \dot{\underline{x}}^T C\ \dot{\underline{x}} = \underline{\eta}^T\ CK^*\underline{\eta} = \underline{q}^T\ \Psi^T CK^*\ \Psi\ \underline{q} \tag{41}$$

with
$$\underline{\eta} = \left\{\begin{matrix}\dot{\underline{x}}\\ \underline{x}\end{matrix}\right\} = \Psi\ \underline{q} = \left\{\begin{matrix}\Phi\ \Lambda\\ \Phi\end{matrix}\right\} \tag{42}$$

Symbolizing aderivative by a comma as $\partial D/C_m \equiv D,_c$ the derivative of Eq. (41) is

$$2\ D,_c = 2\ q^T_{,c}\ \Psi^T CK^* \Psi\ q + 2\ q\ \Psi,_c{}^T\ CK^* \Psi\ q + q\ \Psi^T\ CK^*,_c\ \Psi\ q \qquad (43)$$

Here $q_i = q_i(0)\ e^{-\lambda_i t}$. From Eq. (42) the derivative $\Psi_{,c}$ involves the derivative of the eigenvalues λ_i and the eigenvectors Φ, which may be found by the methods of references 16 through 21.

Next an example of a ten-bar truss is presented, where first the optimization of modal damping ratios is discussed and then the optimization of the energy dissipation rate D is considered.

OPTIMIZATION OF DAMPING RATIO AND DISSIPATION RATE, TEN-BAR TRUSS

The question addressed in this section is: suppose the total dashpot capability, with units of lb-s/in, is limited, then on which members of the truss may it be used most efficiently to maximize the damping ratios, ζ_i, of selected modes? Thus, with α_i appropriate weighting functions, the objective function, OBJ, is

$$OBJ = \sum_i \alpha_i\ \zeta_i . \qquad (44)$$

If CTOT is the total dashpot capacity to be used, then a corresponding constraint equation is

$$G(1) = \sum \gamma_m C_m - \gamma_T CTOT \leq 0.0 \qquad (45)$$

where γ are weighting factors and tC_m are the viscous dashpot constants, taken here as design parameters.

As an example, the ten-bar truss shown in Figure 1 was investigated. The connections are assumed to be frictionless pins. The bars are all made of the same material with Young's modulus E, and the cross-sectional areas A_m are as listed in Table 1. The stiffness of each bar is $K_m = A_m E_m / L_m$. Parallel to each bar there is a dashpot, not shown, with damping parameter C_m. Note that members 2, 5, 6, and 10 have much smaller areas than the other six bars.

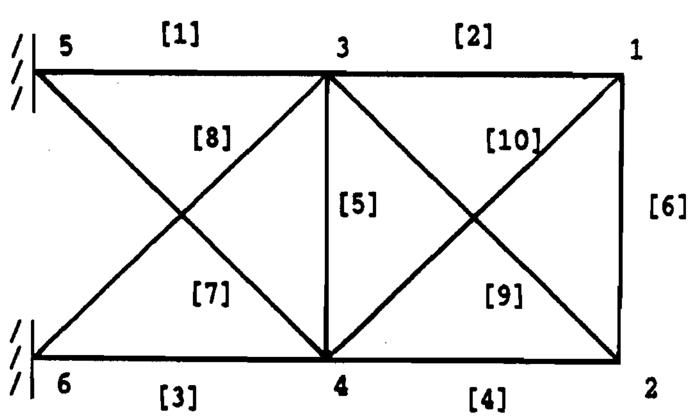

Figure 1 Ten-bar Truss, with Node and Member Numbers

Table 1 Member Areas, Lengths, Stiffnesses and Damping Parameters

El. No. m	Area A_m in	Length L_m in	Stiffness K_m lb/in	Damping C_m (β_m=1) lb s/in
1	31.5	360.000	875 000	276.699 30
2	0.1	360.000	2 778	0.878 41
3	23.0	360.000	638 889	202.034 41
4	15.5	360.000	430 556	136.153 62
5	0.1	360.000	2 778	0.878 41
6	0.5	360.000	4 167	4.392 05
7	7.5	509.117	147 314	46.584 75
8	20.5	509.117	402 658	127.331 65
9	21.0	509.117	412 479	130.437 30
10	0.1	509.117	1 964	0.621 13

A factor β_m is arbitrarily introduced such that $C_m = \frac{\beta_m K_m}{\sqrt{E}}$. Hence if all the β_m are the same, the damping matrix C is proportional to the stiffness matrix K. The mass matrix M is diagonal, formed by lumping half the mass of each bar at its ends. The values of the modal damping ratios, ζ_i, and the natural frequencies, ω_i, are given in Table 2, for the values of C_m when $\beta_m = 1$, for m =1 to 10. The damping ratios for the higher modes are the largest. The ω_i range from 131.13 to 796.21 rad/s and are well separated.

Table 2 Natural Frequencies ω_i and Damping Ratios ζ_i for all β_m=1.0

i	ζ_i	ω_i (rad/s)
1	0.0207 3350	131.1301
2	0.0274 1571	173.3921
3	0.0426 4408	269.7048
4	0.0515 5221	326.0448
5	0.0730 5049	462.0119
6	0.0948 6770	599.9960
7	0.1051 3561	664.9360
8	0.1258 9253	796.2143

The eight mode shapes for zero damping are shown in Figure 2. Intuition tells us that, for a dashpot to be effective: (1) there must be a high relative velocity between the end-points amd (2) it should be in parallel with a bar or relatively small stiffness. The first criterion is satisfied if there is a large extension of the of the bar on the mode shape. Inspection of the shape for mode 2 reveals that bars 2, 5,7 and 10 have large deformations; for mode 4, bars 2 and 10; for mode 7, bars 6 and 10; and so on. If damping is added in a proportional manner, then the mode shapes, or vectors, remain real and the same as shown. If damping becomes nonproportional, the mode shapes do change and eigenvectors contain complex numbers. As the mode shapes change the optimum distribution of the damping to the various members may change from that which was most favorable for small or no damping. This effect is not accounted for in analyses that assume that the damping is proportional. The derivatives $\partial\zeta_i/\partial C_m$ of the ith modal damping with respect to the mth dashpot C_m indicate how ζ_i is changing with increased damping, and the $\partial\varphi_i/\partial C_m$ show the rate of change of the mode shape with the mth dashpot. The derivatives of ζ_i were found and are discussed next.

Sensitivities of Modal Damping Ratios and Natural Frequencies

The exact derivatives $\partial\zeta_i/\partial C_m$ were calculated and their values are listed in Table 3. There are 80 elements, corresponding to 8 modes and 10 bars. The total for each row and column is also given, and these sub-totals add to the grand total of 10.27867. By the sums at the bottoms of the columns, the list of the bars in order of the magnitudes of the sensitivities is 2,10,6,5,4,9,3, 8,1,7. By stiffness, from smallest to largest, the order is 10,2,5,6,7,8,4, 4,3,1. Bar 7 seems to be somewhat out of order, but notice that there are two negative values in the column for bar 7. In a ranking of potential effectiveness according to the absolute sum of the columns, the value for dashpot 7 would be 0.037637 and it would precede dashpot 3 in the sensitivity list.

The fact that negative derivatives occur for bar 7 on modes 1 and 2 shows that the modal damping ratio will decrease for these modes as the value of C_7 is increased. These derivatives were calculated for the damping level where all β_m=1 and the values of the modal damping ratios ζ_i are the same as those given in Table 2. Thus the negative sensitivity has occurred at small levels of damping.

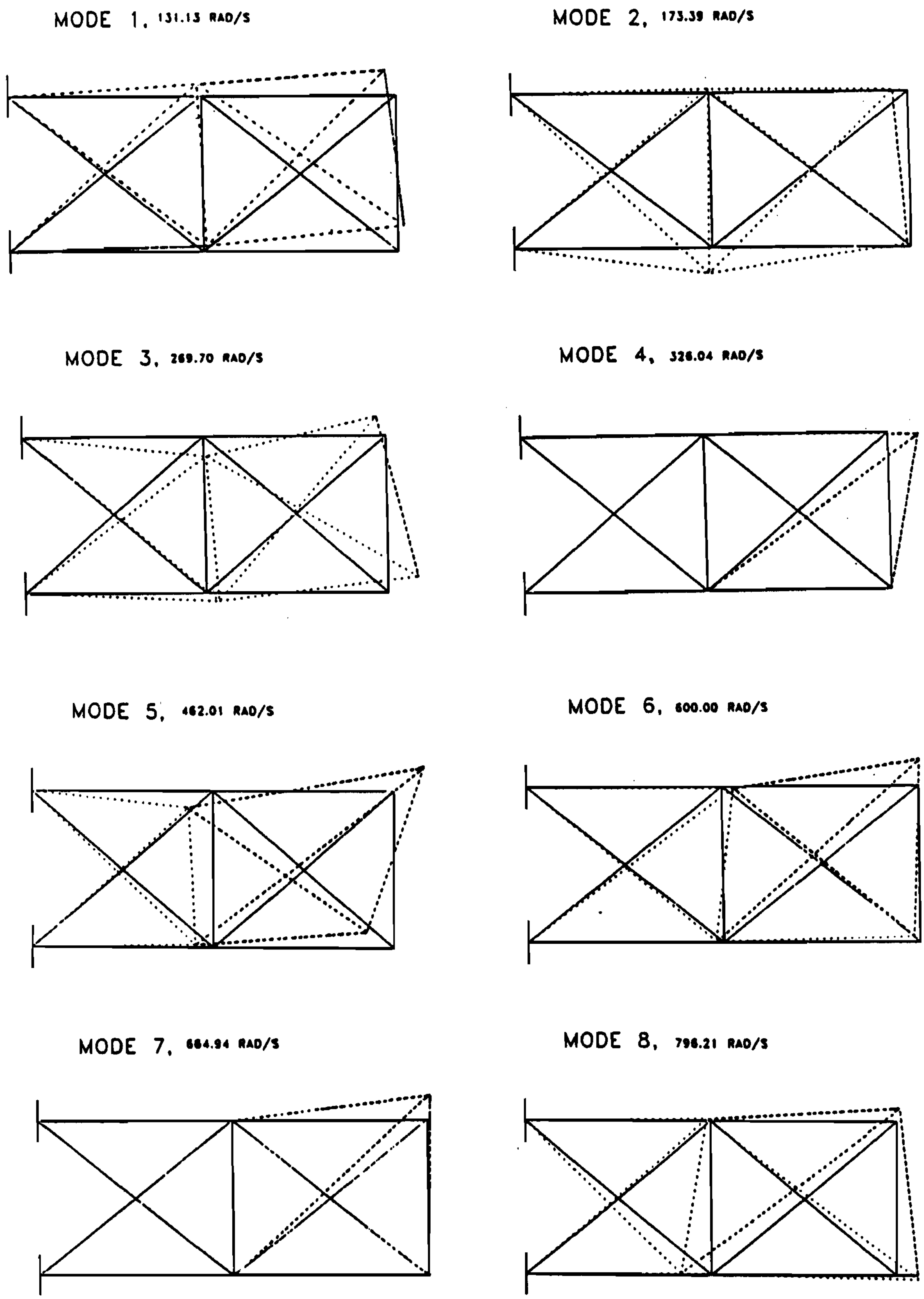

Figure 2 Mode Shapes for Zero Damping

Variation of ζ_5, ζ_6, ω_5, and ω_6 with C_1

As the values of the C_m are changed nonproportionally, the modal amplitudes become complex numbers and the derivatives or gradients change in an unexpected manner in some cases. The variation of ζ_5 and ζ_6 with C_1 is shown in Fig. 3. The values of all other C_m were taken as zero. The plot shows that, for $0 \leq C_1 \leq 3$, both ζ_5 and ζ_6 increase monotonically. However, for $C_1 > 3$, the rate of increase of ζ_6 becomes larger while ζ_5 decreases. The slopes of these lines are plotted in Fig. 4, where it is seen that the $\partial\zeta_5/\partial C_1$ changes sign and finally approaches zero as C_1 increases.

The corresponding variation of the damped natural frequencies ω_{D5} and ω_{D6} with C_1 is shown in Fig. 5. Here ω_{Di} defined as in Eq. (13). Note that ω_{D6} decreases in magnitude while ω_{D5} is increasing. At $\beta_1 \cong 6$, the curves cross and thereafter ω_{D5} approaches a constant value but remains greater than ω_{D6}. As $\beta_1 \cong 12.0$, ζ_6 approaches unity or critical damping as ω_{D6} approaches zero. As β_1 is further increased, the eigenvalues for mode 6 become real and negative, while the other fourteen eigenvalues are still complex conjugate pairs, for underdamped modes. Actually, if the modes are numbered initially in terms of the magnitude of ω_{Di}, from smallest to largest, then it is clear that they will change their relative positions as the damping increases. Hence their identities must be traced carefully if changes in a mode having a particular "name" are of interest. The tracing of mode numbers is especially challenging when more than one mode is overdamped, since they no longer occur in complex conjugate pairs.

Optimization of ζ_3 with Respect to C_3 and C_4.

Now the optimization of one modal damping ratio is undertaken, with the objective function taken as ζ_3 and the design variables C_3 and C_4. Constraint function G(1) puts a limit CTOT on the total damping available.

$$OBJ = \zeta_3$$

$$G(1) = C_3 + C_4 - CTOT \leq 0.0 \tag{46}$$

By limiting the total number of design variables to two, we can show a two-dimensional plot of the interaction between ζ_3 and the two design variables. Contours for $\zeta_3 = 0.05, 0.10, 0.15,$ and 0.20 are shown in Figure 6. The three dotted, straight lines are constraint lines which were chosen to be approximately tangent to the given contour lines. They would be 45° lines if the vertical and horizontal scales were equal. Since the contours are convex toward the feasible region the optimum solution, which maximizes ζ_3, will be along the constraint boundary line. The results are summarized in Table 4 for three values of CTOT, namely CTOT = 1157.3, 1838.5, and 2525.4 lb-s/in. The associated values of optimum ζ_3 are close to 0.10, 0.15 and 0.20.

Table 4 Optimum Values of ζ_3 on C_3 vs. C_4 Plot

β_3	β_4	C_3	C_4	ζ_3	C_3+C_4
0.796 537	7.318	160.928	996.373	0.0994 4614	1157.301
3.560 435	8.22	719.330	1119.184	0.1470 4782	1838.514
6.142 305	9.434	1240.957	1284.475	0.2015 5902	2525.432

Optimization of 2D(0) for Mode 3 using parameters C_3 and C_4

Next the dissipation rate at t=0, 2D(0), was optimized when only mode 3 is excited in free vibrations by taking $q_3(0)= \bar{q}_3(0) =1.0$. The interaction curves of contours of 2D(0) on a plot of C_3 versus C_4 are shown in Figure 6. The curved contour lines are for 2D(0)= 50, 100, 150, and 200 in-lb/s. The solid, straight, constraint line represents the constraint $C_3 + C_4 \leq 1040$, and the region between this line and the coordinate axes includes feasible, or acceptable solutions, as specified by the constraint equation. Obviously the optimum solution is at the point of tangency between the constraint boundary and a contour line, which occurs approximately at C_3= 860 and C_4= 860 lb-s/in.

Optimization of 2D(0) for modes 4 and 7 using parameters C_6 and C_{10}

In Figures 8, 9, and 10 three more interaction curves, each of a different shape, are shown for 2D(0). They are for modes 4 and 7 excited separately and simultaneously, with the contours of 2D(0) plotted against C_6 versus C_{10}. In each case the contours are either nearly straight lines, as in Figure 8 and 9, or outwardly convex curves, as in Figure 10. In these situations, the optimum solution is seen to be a corner of the feasible region, with the solutions for the design parameters being C_6=0, C_{10}=8.3; C_6=8.3, C_{10}=0; and C_6=0, C_{10}=8.3 on the respective Figures 8, 9 and 10.

Table 4 Sensitivities $\frac{\partial \zeta_i}{\partial C_m} \times 10^2$

At C_m as given in Table 1

Mode No. i \ Bar No. m →	1	2	3	4	5
1	0.002 025	0.004 389	0.000 900	0.001 138	0.007 674
2	0.000 197	0.021 051	0.001 518	0.000 001	0.154 036
3	0.000 180	0.004 650	0.005 255	0.010 230	0.006 373
4	0.000 054	4.336 10	0.000 037	0.000 021	0.000 486
5	0.008 992	0.045 043	0.004 783	0.001 471	0.007 432
6	0.011 616	0.009 531	0.005 680	0.000 325	0.000 890
7	0.000 203	0.018 862	0.000 531	0.000 367	0.000 079
8	0.000 314	0.000 946	0.017 544	0.051 749	0.000 016
	0.023 581	4.440 572	0.036 248	0.065 302	0.176 986

i \ m →	6	7	8	9	10	All
1	0.000 035	-0.001 810	0.006 954	0.001 747	0.007 211	0.030 263
2	0.000 238	-0.012 466	0.000 762	0.000 059	0.029 303	0.194 699
3	0.000 355	0.006 633	0.007 399	0.003 263	0.001 391	0.045 729
4	0.033 031	0.000 104	0.000 117	0.000 000	1.853 09	6.223 04
5	0.001 360	0.003 230	0.014 265	0.012 294	0.039 581	0.138 451
6	0.069 406	0.003 364	0.003 603	0.031 427	0.081 899	0.217 741
7	2.122 32	0.000 344	0.000 039	0.001 667	1.164 52	3.308 932
8	0.007 902	0.009 686	0.000 024	0.010 797	0.020 834	0.119 812
	2.234 647	0.009 085	0.033 163	0.061 254	3.197 829	10.278 67

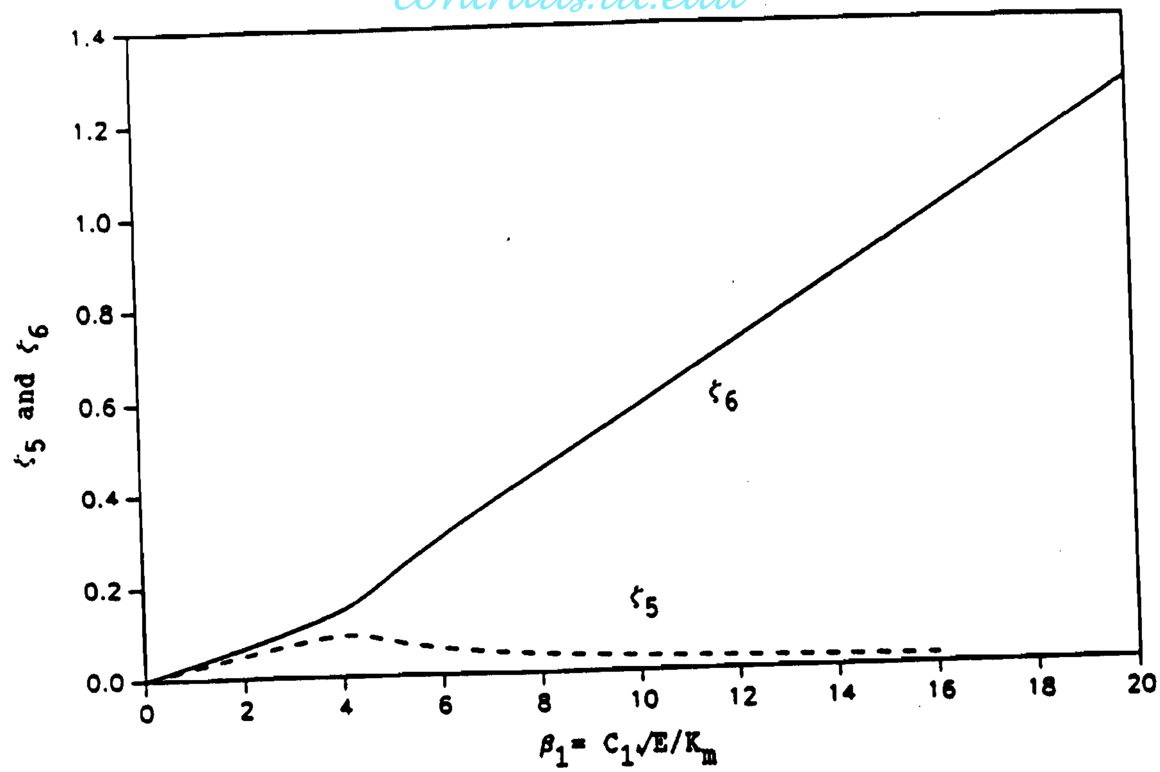

Figure 3 Modal damping ratios, ζ_5 and ζ_6 versus C1.

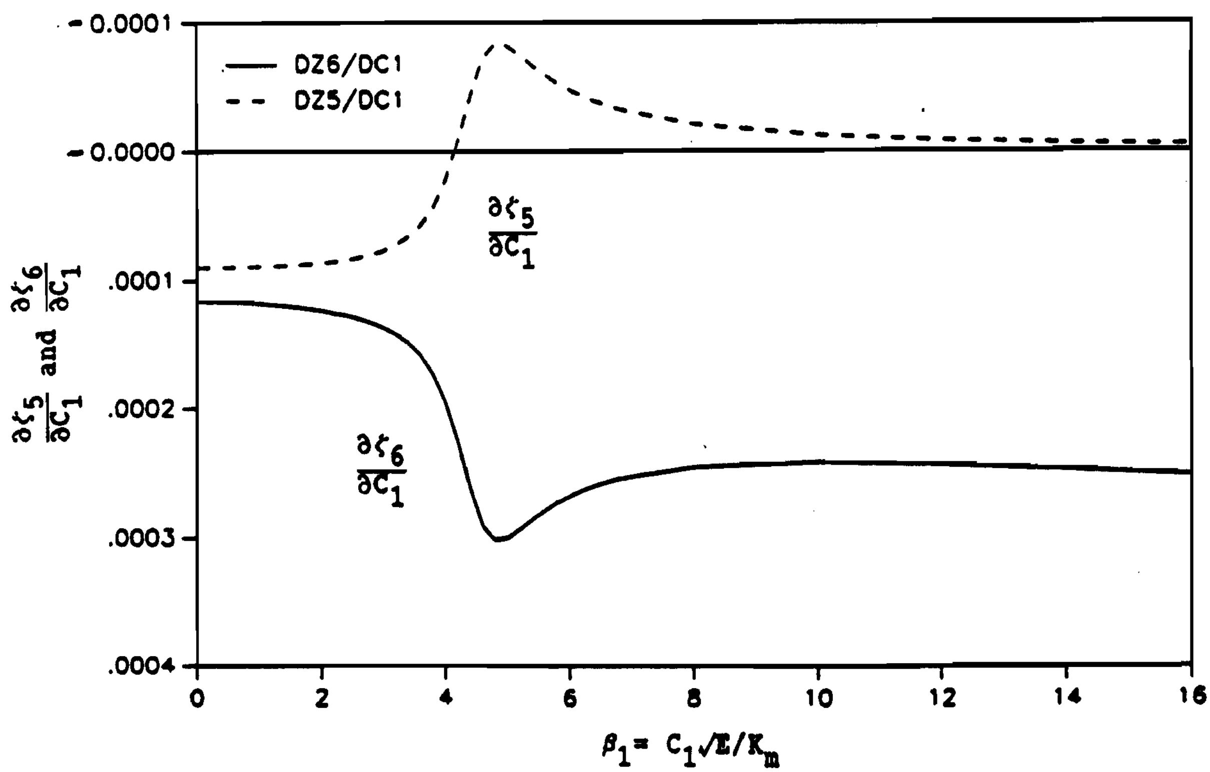

Figure 4 Sensitivities, $\frac{\partial\zeta_5}{\partial C_1}$ and $\frac{\partial\zeta_6}{\partial C_1}$, versus β_1.

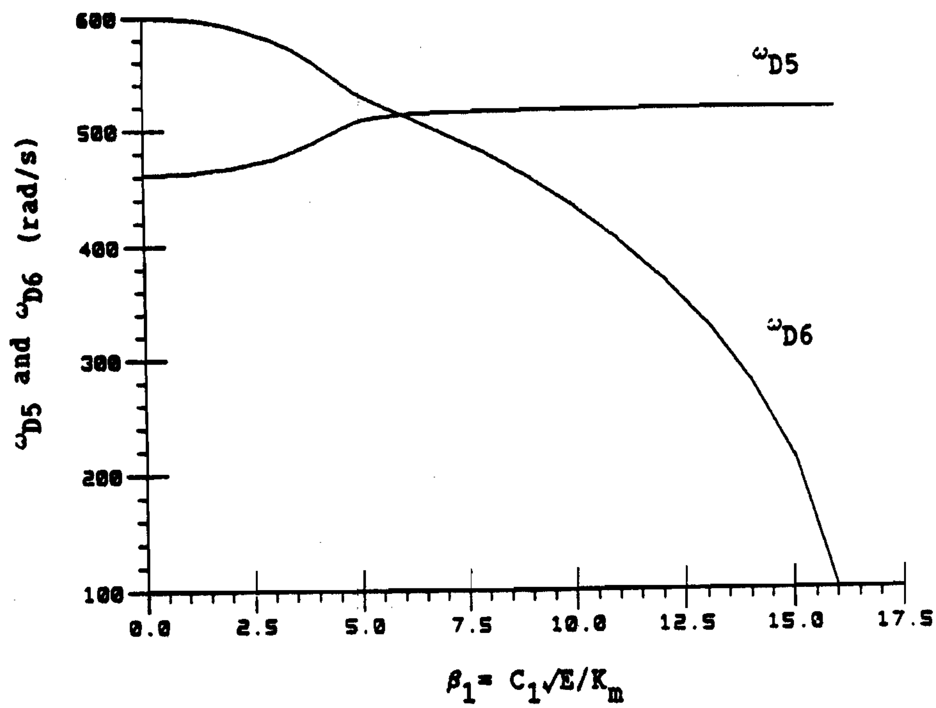

Figure 5 Damped Natural Frequencies ω_{D5} and ω_{D6} versus β_1.

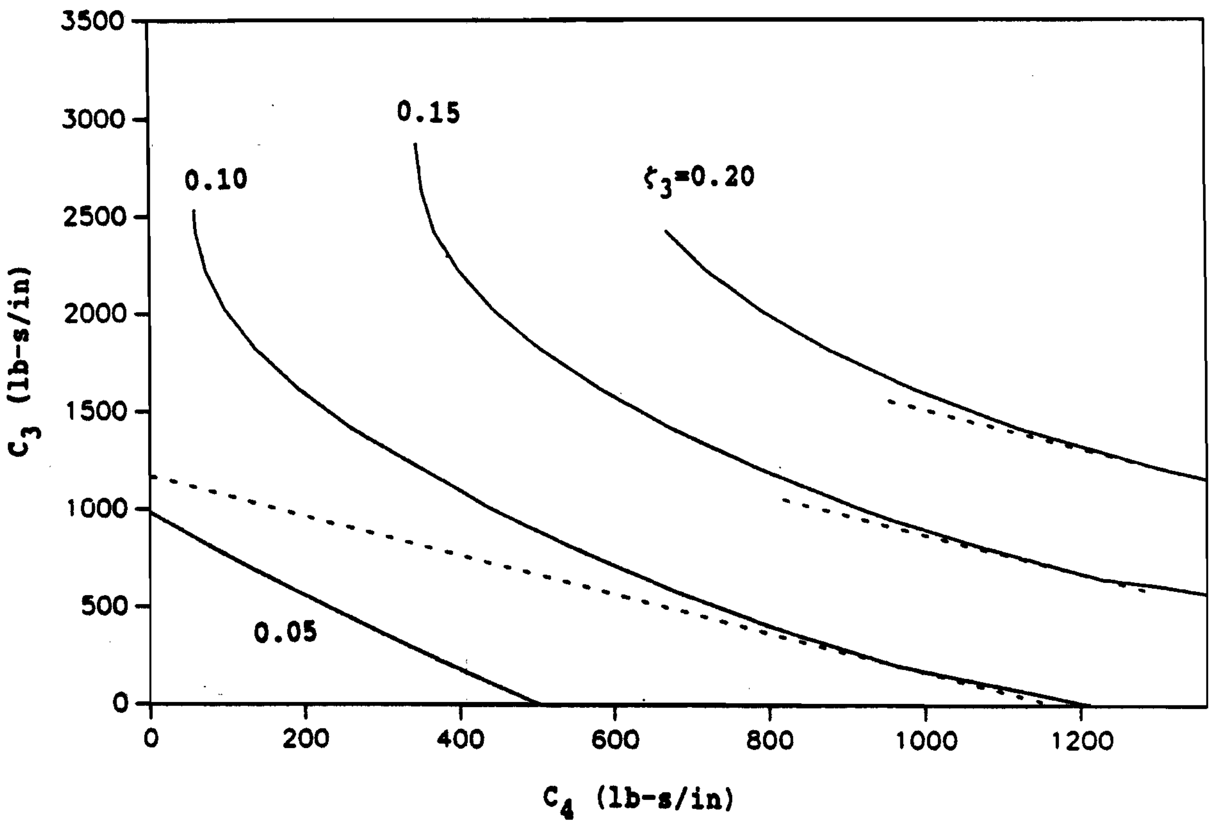

Fig. 6. Interaction of ζ_3 with C_3 and C_4, with Constraint Boundaries (Dotted)

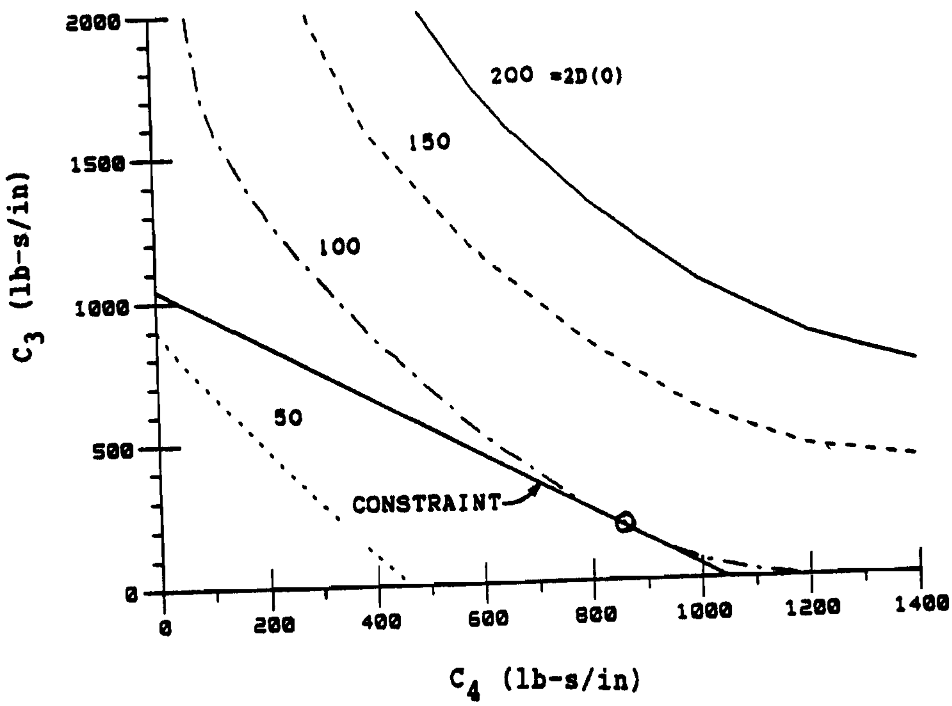

Figure 7 Interaction of 2D(0) with C3 and C4, Mode 3 Excited.

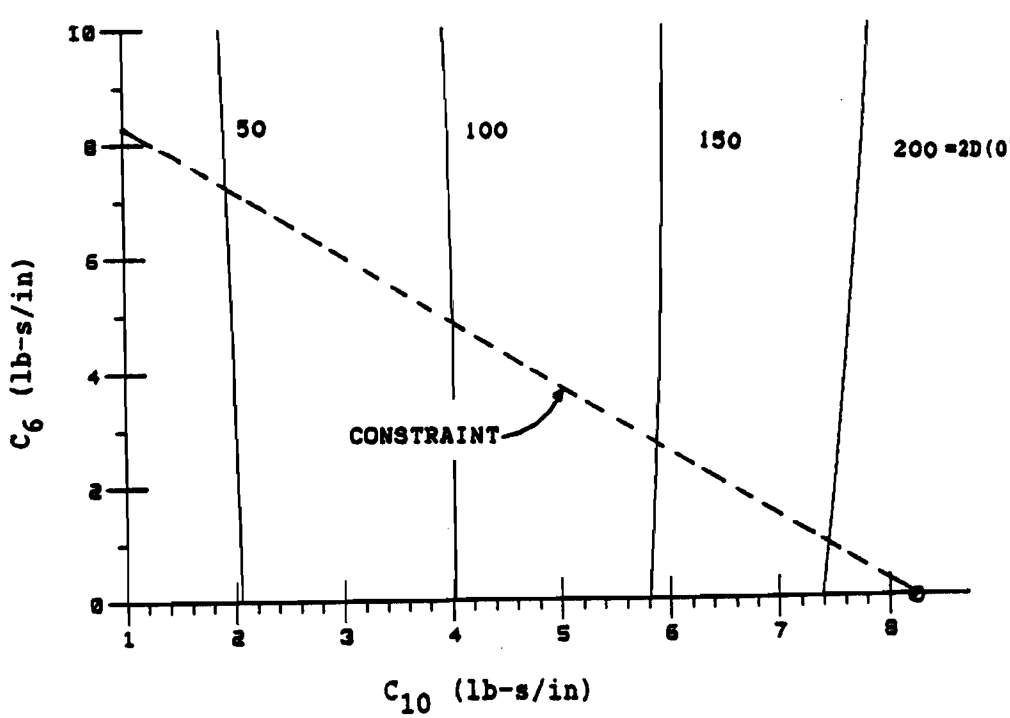

Figure 8 Interaction of 2D(0) with C_6 and C_{10}, Mode 4 Excited.

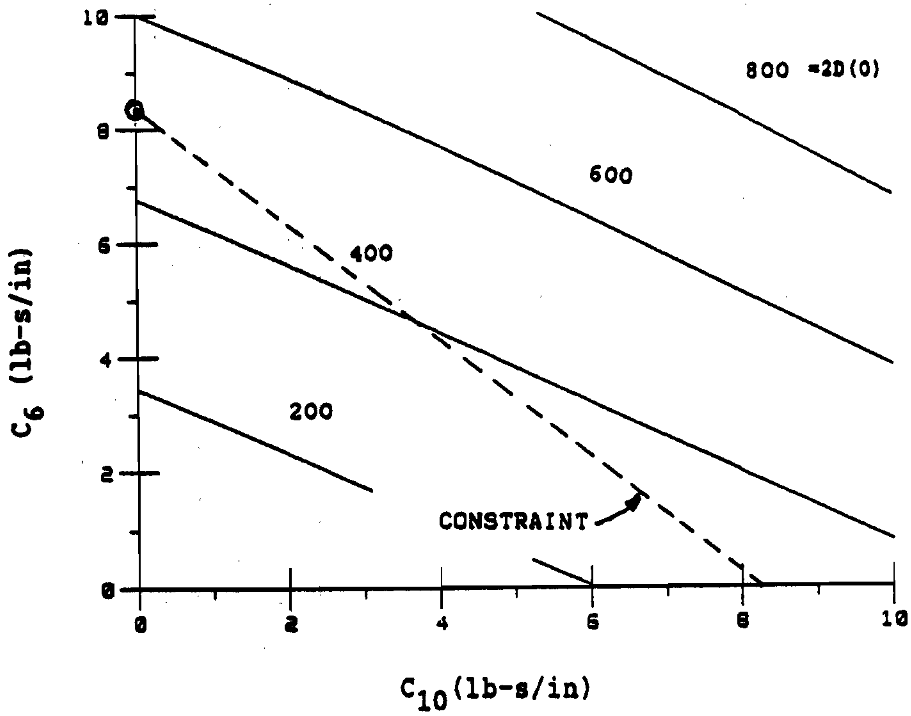

Figure 9 Interaction of 2D(0) with C_6 and C_{10}, Mode 7 Excited.

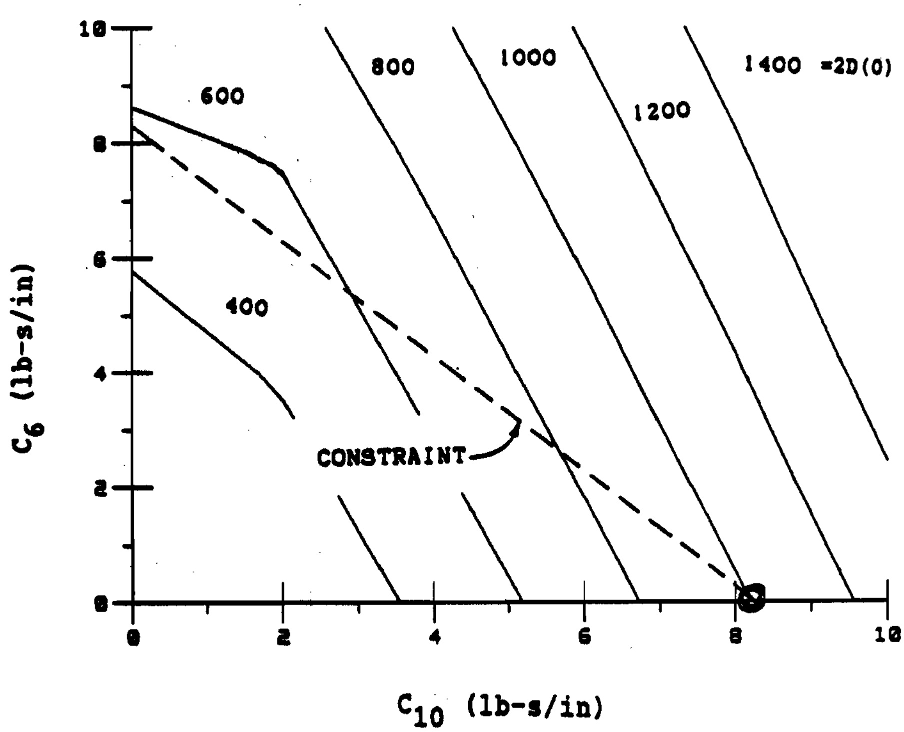

Figure 10 Interaction of 2D(0) with C_6 and C_{10}, Modes 4 & 7 Excited.

Timewise Variation of the Dissipation Rate 2D(t) for Modes 5 and 6

The timewise variations of the energy dissipation rate for modes 5 and 6 excited separately and simultaneously are shown in Figures 11 and 12, for proportional and nonproportional damping respectively. In Figure 11 the solid curve is for modes 5 and 6 excited simultaneously and the two other lines are for modes 5 and 6 excited separately. The solid line seems to be a sum of the other two. In Figure 11, for nonproportional damping, where β_1=1.0 and all other β_m=0, the case is entirely different and the dissipation rate at t=0 for the simultaneous excitation of modes 5 and 6 is almost double that achieved by excitation of the modes individually. This is because, as mentioned above, the core matrix used for solving for the dissipation rate is nondiagonal, and the additional contribution is due to nondiagonal, or modal cross-product elements contributing to the dissipation rate. In Table 5, a portion of this matrix is shown for the rows and columns involving modes 5 and 6. Mode 5 would be excited by making the initial values $q_5(0) = q_5(0)$ = 1.0, or simply inserting ones for q_5 and q_6 in the given matrices. It can be seen that the resulting value of 2D(0) is equal to the sum of the complex numbers in the upper corner, 2x2, of this portion of the matrix. Here the notation is: (a,b) = (a+jb). So the value of 2D(0) with only mode 5 excited is the real number 46.64 in-lb/s. If only mode 6 is excited, the numbers in the lower corner 2x2 are summed to yield 78.68 in-lb/s. If the two modes are excited simultaneously, the entire 4x4 matrix is summed for a total of 246.49 in-lb/s, which is almost twice the total obtained by exciting the modes individually. In Table 6 the values of the kinetic and potential energies, T and U, and their timewise derivatives at t=0 are also given. Note that $\dot{T}(0)+\dot{U}(0)+2D(0) = 0$ and $T(0)-U(0) = 2n$, as expected, where n is the number of modes excited. The ratio $2D(0)/[T(0)+U(0)]$ is meaningful because it is the ratio of the dissipation rate to the total initial energy excited. From this point of view, for proportional damping, the

Table 5 Portion of core of $\Lambda^T\Phi^T C\Phi\Lambda$ complex matrix.

$(q_5\bar{q}_5q_6\bar{q}_6)$	(11.52,-2.54)	(11.80,-0.00)	(15.32,-0.02)	(14.97,-3.28)	q_5
	(11.80, 0.00)	(11.52, 2.54)	(14.97, 3.28)	(15.32, 0.02)	$\bar{q}_5$
	(15.32,-0.02)	(14.97, 3.28)	(19.44, 4.23)	(19.90, 0.00)	q_6
	(14.97,-3.28)	(15.32, 0.02)	(19.90, 0.00)	(19.44,-4.23)	$\bar{q}_6$

Table 6 Energies and Energy Rates, Prop. and Nonprop. Damping

Modes Excited	T(0)	U(0)	$\dot{T}(0)$	$\dot{U}(0)$	2D(0)	$\frac{2D(0)}{T(0)+U(0)}$
Proportional Damping, β_m= 1.0, all β_m.						
5	2.0027	0.0027	-101.34	-33.84	135.18	67.41
6	2.0045	0.0045	-171.02	-57.18	228.20	113.59
5&6	4.0072	0.0072	-272.36	-91.02	363.38	90.52
Nonproportional Damping, β_1 = 1.0, β_m = 0.0, m ≠ 1.						
5	2.0317	0.0317	- 34.83	-11.82	46.64	22.60
6	2.0228	0.0228	- 58.68	-20.00	78.68	38.46
5&6	4.0605	0.0605	-154.09	-92.40	246.49	59.82

ratio is largest if mode 6 is excited by itself, but for nonproportional damping the ratio is more favorable if modes 5&6 are excited simultaneously.

It should be noted with regard to Table 5 that here all the real parts of the complex numbers are positive. This is not true of the entire core matrix in general, and it may be necessary to excite the modes with varying initial phase to achieve the maximum damping rate, and the rate achieved in this manner may still be somewhat less than ||Core||, herein defined as the sum of the absolute values of the real numbers in the core matrix.

Sensitivity of ||Core|| to parameters C_m

Finally the sensitivity of ||Core|| to changes in C_m as found by the finite difference method are given in Table 7. In each case, the initial C_m= 1.0 and ΔC_m=0.10. The largest gradients occur for the dashpots 2, 6, and 10.

Table 7 Sensitivity of ||Core|| to ΔC_m

m	C_m	||Core||	$\frac{\Delta\|\|Core\|\|}{\Delta C_m}$
1	1	1.74	1.74
2	1	110.77	109.56
3	1	3.86	3.86
4	1	4.26	4.26
5	1	4.67	4.67
6	1	103.89	101.88
7	1	4.69	4.69
8	1	2.11	2.11
9	1	6.01	6.01
10	1	204.91	204.47

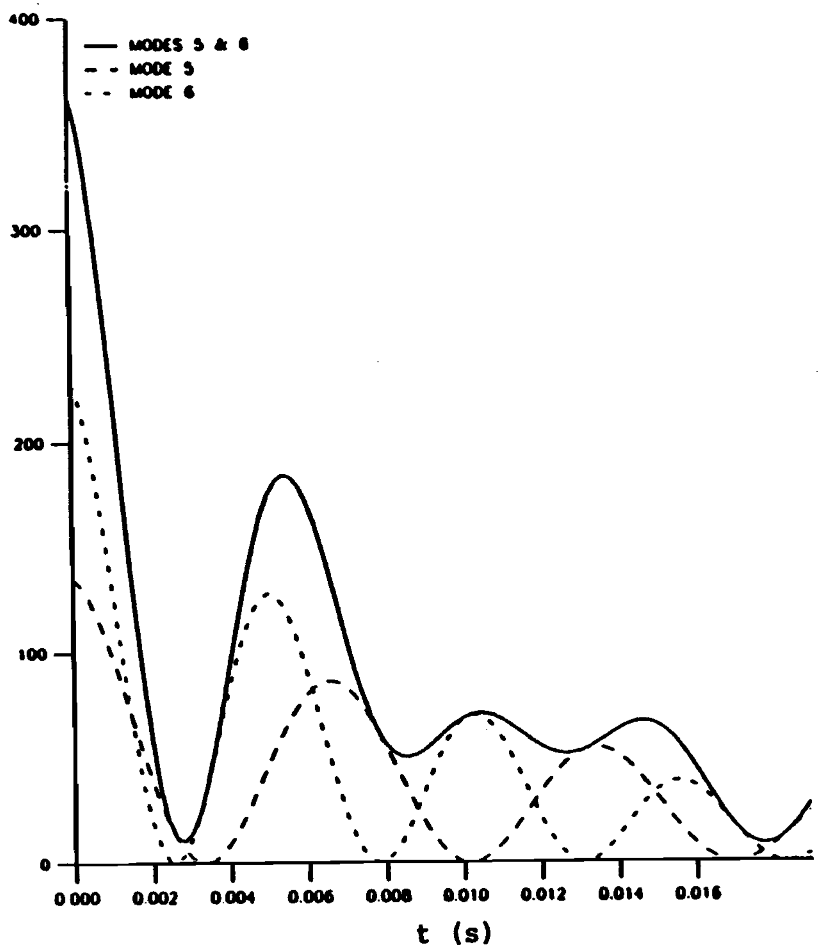

Figure 11 2D(0) versus Time, All β =1.0.
Proportional Damping
Modes 5, 6 and 5 & 6.

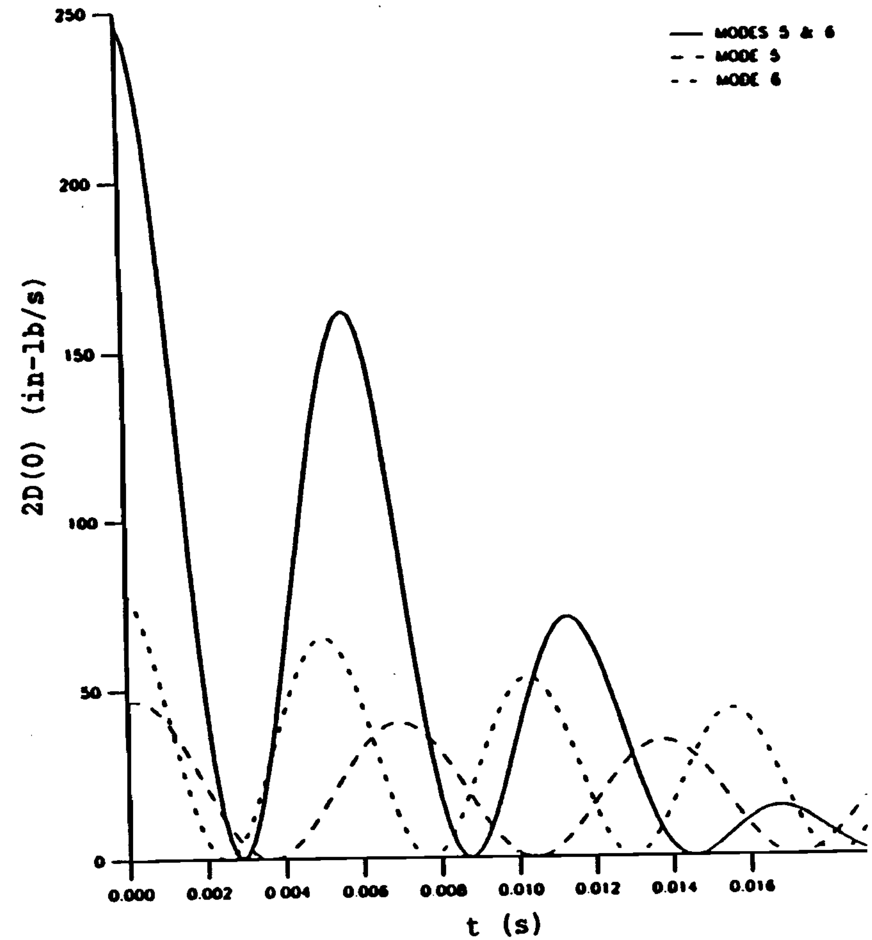

Figure 12 2D(0) versus Time, Only β_1 =1.0.
Nonprortional Damping
Modes 5, 6 and 5 & 6.

Summary and Conclusions

1. It is demonstrated that the energy dissipation rate may be optimized simply by using its value at time t=0 as the cost function. The settling time depends on the total initial energy, which is the sum of the initial kinetic and potential energies T(0) and U(0) and the dissipation rate 2D(0).

2. Because of the modal normalization procedure used in the present work, the sum T(0)-U(0)=2n, where n is the number of modes excited with unit amplitude. In the examples given, the U(0) was much smaller than T(0), so the total initial energy equals T(0) and $T(0) \cong 2n$.

3. An upper bound on the maximum energy dissipation rate which may be achieved, if all the modes are excited with unit amplitude, is equal to the sum of the absolute values of real parts of the complex numbers in the CORE of the matrix from which 2D is calculated, which is

$$2D = \underset{\sim}{q}^T \Lambda^T \Psi^T C K^* \Psi \Lambda \underset{\sim}{q} = \underset{\sim}{q}^T \text{ CORE } \underset{\sim}{q}$$

If desired, the individual modes may be weighted differently when excited, to put more emphasis on modes of interest. In a practical problem, the initial values $\underset{\sim}{q}(0)$ could be taken as those which actually exist.

4. The derivative, or sensitivity, of the Core to the damping paramters may be calculated by taking the derivative of the given expression, which is seen to involve the derivatives of the eigenvalue and eigenvector matrices, Λ and Ψ, as well as the damping matrix C.

5. The problem of deciding which truss members to damp and how much damping to use is reduced to a standard optimization problem. This problem may be solved by the Method of Steepest Descent or the Method of Feasible Directions. The solution may be obtained using a computer program such as CONMIN, which has been used by the writer to minimize the forced random response of the given truss while maintaining constraints on the modal damping ratios, so the damping is evenly distributed to the modes.

6. Study of the sensitivities of the damping ratios and damped natural frequencies of free vibration shows that as the viscous damping of a particular dashpot is increased, the damping ratio of one mode may decrease while the damping ratios of the other modes is increasing. Concurrently, the damped natural frequency of that one mode will be increasing while that of the other modes is decreasing. In the example given, one mode finally absorbed all the damping provided. Thus, in a practical situation, it appears possible that in some rare situations increasing damping could make matters worse, if damping is decreasing in the mode or modes that are being excited. The effect described is due to change in mode shape.

Acknowledgments

The benefit of discussion with Dr. V. B. Venkayya, V. Tischler, D. Veley R. Kolonay, Capt. R Canfield, and Dr. L. Rogers of Wright-Patterson Air Force Base is gratefully acknowledged.

References

1. NASA/DOD Control/Structures Interaction Technology, NASA CP 2447, Parts 1 and 2, 1986.

2. Carne, T. G., and Simonis, J.C., Editors, Modal Testing and Analysis, ASME DE-Vol. 3, Sept., 1987.

3. Rogers, L. and Simonis, J. C., Editors, The Role of Damping in Vibration and Noise Control, ASME DE-Vol.4, Sept., 1987.

4. Inman, D. J. and Simonis, J. C., Editors, Vibration Control and Active Vibration Suppression, ASME DE-Vol.5, Sept., 1987.

5. Leipholz, H. H. E. and Abdel-Rohman, Control of Structures, Martinus Nijhoff Publ, Boston and Lancaster, and Kluwer Acad. Publ., Hingham, MA 1986.

6. Meirovitch, L., Introduction to Dynamics and Control, Wiley, NY, 1985.

7. Neubert, V. H., Impedance: Modelling/Analysis of Structures, Jostens Publ. Co., State College, PA, 1988.

8. Nashif, A. D., Jones, D.I.G., and Henderson, R. P., Vibration Damping, Wiley, New York, 1985.

9. Soovere, J. and Drake, M.L., Aerospace Structures Technology Damping Design Guide, Vol. I-Technology Review, Vol. II-Design Guide, Vol. III- Damping Material Data, AFWAL-TR-84-3089, December 1985.

10. Bagley, D.L. and Torvik, P.J., "Fractional Calculus-A Different Approach to the Analysis of Viscoelastically Damped Structures", AIAA Journal, v.21, n.5, pp. 741-748, 1983.

11. Segalman, D.J., "Calculation of Damping Matrices for Linearly Viscoelastic Structures," Journal of Applied Mechanics, v. 54, pp.585-588, Sept, 1987.

12. McTavish, D.J. and Hughes, P.C., "Finite Element Modeling of Linear Viscoelastic Structures," in Ref. 3, pp. 9-18.

13. Venkayya, V. B., "Optimality Criteria: A Basis for Multidisciplinary Design Optimization," Computational Mechanics, 1988.

14. Vanderplaats, G. N., "CONMIN - A Fortran Program for Constrained Function Minimization, User's Manual," NASA(Ames)TMX-62,282, Aug 1973 and CONMIN User's Manual Addendum", May 1978.

15. Rogers, L. C., "Derivatives of Eigenvalues and Eigenvectors", AIAA Journal, v. 8, pp. 943-944, May 1970.

16. Nelson, R. B., "Simplified Calculation of Eigenvector Derivatives," AIAA Journal, v.14, n.9, pp. 1201-1205, Sept. 1976.

17. Sutter, T. R., Carmarda, C. J., Walsh, J. L., and Adelman, H. M., "A Comparison of Several Methods for the Calculation of Vibration Mode Shape Derivatives", Proc. AIAA/ASME/ASCE/AHS 27th Structures, Structural Dynamics and Materials Conference, San Antonio, TX, May 1986.

18. Lim, K. M., Junkins, J. L., and Wang, B. P., "Re-examination of Eigenvector Derivatives," Rev. Received AIAA Journal, Feb. 20, 1987.

19. Ojalvo, I. U., "Efficient Computation of Mode-Shape Derivatives for Large Dynamic Systems", AIAA Journal, v. 25, n. 10, 1986.

20. Fetterman, T. L. and Noor, A.K., "Computational Procedures for Evaluating the Sensitivity Derivatives of Vibration Frequencies and Eigenmodes of Framed Structures", NASA CR 4099, 1987.

21. Gibson, W. C. and Johnson, C. D. "Optimization Methods for Design of Viscoelastic Damping Treatments", In Reference 3, pp. 279-286.

22. Crandall, S. H. and McCalley, R.B., "Numerical Methods of Analysis," in Harris, C. M. and Crede, C.E., Shock and Vibration Handbook, McGraw-Hill, Inc. 1961.